

# Classification of Photometric Factors Based on Photometric Linearization

Yasuhiro Mukaigawa\*<sup>1</sup>, Yasunori Ishii\*<sup>2</sup>, and Takeshi Shakunaga<sup>3</sup>

<sup>1</sup> The Institute of Scientific and Industrial Research, Osaka University  
8-1 Mihogaoka, Ibaraki-shi, Osaka 567-0047, JAPAN

`mukaigaw@am.sanken.osaka-u.ac.jp`

<sup>2</sup> Matsushita Electric Industrial Co., Ltd.

<sup>3</sup> Department of Computer Science, Okayama University  
Okayama-shi, Okayama 700-8530, JAPAN

**Abstract.** We propose a new method for classification of photometric factors, such as diffuse reflection, specular reflection, attached shadow, and cast shadow. For analyzing real images, we utilize the photometric linearization method which was originally proposed for image synthesis. First, we show that each pixel can be photometrically classified by the simple comparison of the pixel intensity. Our classification algorithm requires neither 3D shape information nor color information of the scene. Then, we show that the accuracy of the photometric linearization can be improved by introducing a new classification-based criterion to the linearization process. Experimental results show that photometric factors can be correctly classified without any special device.

## 1 Introduction

The appearance of an object changes due to lighting direction and surface reflectance. Since real images include complex factors such as specular reflections and shadows, it is difficult to directly apply various computer vision algorithms, such as photometric stereo[1], to real images. Therefore, it is important to analyze the photometric factors included in real images.

A lot of methods have already been proposed for separating photometric factors. The dichromatic reflection model [2] is often used for separating diffuse reflections and specular reflections [3–5]. Wolff et al.[6] proposed a method to separate specular reflections by analysis of reflected polarization, Nayar et al.[7] combined color and polarization to separate specular reflections. Ikeuchi et al.[8] proposed a method to classify photometric factors based on range and brightness images. These methods, however, have a common restriction in that shadows cannot be analyzed.

On the other hand, there are some methods which express real images in a linear subspace. Shashua[9] showed that an image lighted from any direction can be expressed by a linear combination of three base images taken under different lighting directions under the assumption of a Lambertian surface and a parallel

---

\* This work was mainly accomplished when the authors were with Okayama University.

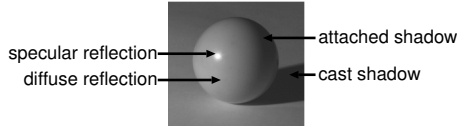


**Fig. 1.** Photometric factors included in an image.

ray. That is, an image can be perfectly expressed in a 3-D subspace. Belhumeur and Kriegman[10] showed that an image can be expressed by the illumination cone model even if the image includes attached shadows. In the illumination cone, images are expressed by a linear combination of extreme rays. Georgiades et al.[11] developed the illumination cone so that cast shadows can be also expressed by the shape reconstruction. Although any photometric factors can be ideally expressed by the illumination cone, a large number of images corresponding to extreme rays are necessary.

We have proposed the photometric linearization method[12], which converts real images into ideal images that include only diffuse factor. After the photometric linearization, all images are expressed as a linear combination of three base images. The method was originally proposed for image synthesis. In this paper, we show that the method can also be used for classifying photometric factors. It can classify not only diffuse reflections and specular reflections, but also attached shadows and cast shadows. We present a new criterion for classification of photometric factors based on the photometric linearization. The classification algorithm requires neither 3D shape information nor color information of the scene. The classification is accomplished by the simple comparison of pixel intensities.

Moreover, we show that the accuracy of the original photometric linearization can be improved by introducing a new classification-based criterion to the linearization process. The original photometric linearization method does not work stably when pixels are not illuminated in a number of input images. Our physics-based analysis can solve this problem.

## 2 Classification

### 2.1 Photometric Factors

Photometric factors are classified into reflections and shadows (Fig.1). The reflections are classified into diffuse reflections and specular reflections. According to the Lambert model, the intensity of the diffuse reflection is expressed by

$$i = \mathbf{n}^T \mathbf{s}. \quad (1)$$

Here,  $\mathbf{n}$  denotes the surface property vector which is a product of the unit normal vector and the diffuse reflectance, and  $\mathbf{s}$  denotes the lighting property vector which is a product of the unit vector along the lighting direction and the lighting power. The specular reflections are observed as the sum of diffuse factors and specular factors.

Shadows are classified into attached shadows and cast shadows. Attached shadows depend on the angle between the surface normal and the lighting direction and are observed where the surface does not face the light source. Cast shadows depend on the overall 3-D shape of the scene, and are observed where light is occluded by other objects. If there is no ambient light and interreflection, the intensity in shadows becomes zero. However, Eq.(1) indicates that the intensity in attached shadow is negative, while that in cast shadow is positive.

## 2.2 Photometric Linearization

We have proposed the photometric linearization method[12] which converts real images including various photometric factors into ideal images including only diffuse reflection factor. After the photometric linearization, all pixels in images fully satisfy Eq.(1). Hence, any image can be expressed by a linear combination of three base images[9].

For the photometric linearization, multiple images are taken under various lighting directions. The camera and target objects are fixed. It is important that the lighting direction, the 3-D shape of the target objects, and the reflectance of the surface are unknown.

## 2.3 Criterion for Classification

In this section, we show that each pixel can be easily classified into diffuse reflection, specular reflection, attached shadow, and cast shadow based on the photometric linearization. The classification is accomplished by the simple comparison of the pixel intensity.

Let  $i_{(k,p)}$  be the intensity of the pixel  $p$  in the image  $k$ , and let  $i_{(k,p)}^L$  be the linearized intensity. The relationship between  $i_{(k,p)}$  and  $i_{(k,p)}^L$  is as follows. In the diffuse reflection region,  $i_{(k,p)}^L$  is equal to  $i_{(k,p)}$ , because the intensity is not changed by the linearization. In the specular reflection region,  $i_{(k,p)}^L$  is smaller than  $i_{(k,p)}$ , because the specular factor is eliminated. In the attached shadow region,  $i_{(k,p)}^L$  becomes negative, which satisfies Eq.(1). In the cast shadow region,  $i_{(k,p)}^L$  is larger than  $i_{(k,p)}$ , because  $i_{(k,p)}^L$  has a diffuse reflection factor while  $i_{(k,p)}$  is near zero. Hence, each pixel can be classified by the following criterion:

$$\begin{aligned}
 & \text{Region}(k,p) = \\
 & \begin{cases} D : \text{if } (|i_{(k,p)} - i_{(k,p)}^L| \leq T \times i_{(k,p)}) \cap (i_{(k,p)} \geq T_s) \\
 S : \text{if } (i_{(k,p)} - i_{(k,p)}^L > T \times i_{(k,p)}) \cap (i_{(k,p)}^L \geq 0) \cap (i_{(k,p)} \geq T_s) \\
 A : \text{if } (i_{(k,p)}^L < 0) \cap (i_{(k,p)} < T_s) \\
 C : \text{if } (i_{(k,p)}^L \geq 0) \cap (i_{(k,p)} < T_s) \\
 U : \text{otherwise} \end{cases} \quad (2)
 \end{aligned}$$

Here,  $D, S, A, C$ , and  $U$  denote diffuse reflection, specular reflection, attached shadow, cast shadow, and undefined factor, respectively. The threshold  $T$  is used to check the equality of  $i_{(k,p)}$  and  $i_{(k,p)}^L$ , and empirically determined. Since

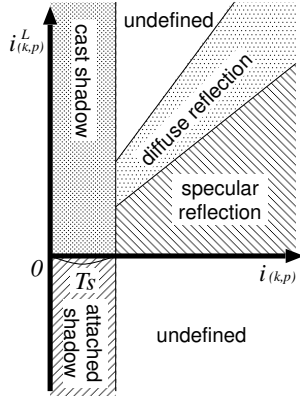


**Fig. 2.** Criterion for classification of photometric factors.

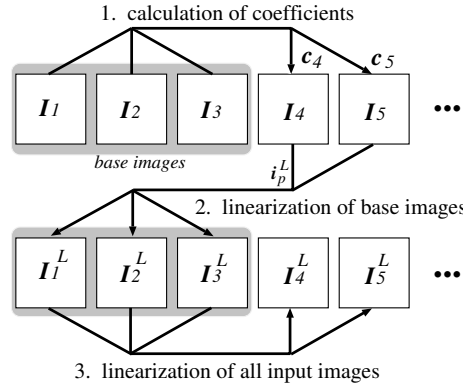


**Fig. 3.** Flow of the linearization process.

$T$  is normalized to be relative to  $i_{(k,p)}$ , the check becomes independent of the brightness. In real images, the intensities of shadows are not zero. The threshold  $T_s$  is used to distinguish shadows, and can be determined by manually sampling some pixels in shadow regions.

In this criterion, the shadow regions are classified just by using threshold  $T_s$ . Although the classification is very simple, attached shadows and cast shadows can be distinguished by the sign of  $i_{(k,p)}^L$ . It is one of the significant advantages of the criterion because two types of shadows can be distinguished without any 3D shape information. Figure 2 illustrates Eq.(2) as a 2-D plane spanned by  $i_{(k,p)}$  and  $i_{(k,p)}^L$ . The photometric factors are easily classified if the photometric linearization is accomplished.

### 3 Improvement of Photometric Linearization

#### 3.1 Key Idea

In the previous section, we showed that photometric factors are correctly classified if the photometric linearization is perfectly accomplished. That is, any pixel is never classified into the undefined factor. This fact suggests that the photometric linearization becomes more accurate by introducing the criterion for classification to the linearization process. We can use the criterion to verify the accuracy of the photometric linearization.

#### 3.2 Flow of the Process

First, we summarize the photometric linearization. Shashua[9] showed that if a parallel ray is assumed, an image  $I_k$  under any lighting direction can be expressed by a linear combination of three base images ( $I_1$ ,  $I_2$ , and  $I_3$ ) taken under different lighting directions,

$$I_k = c_k^1 I_1 + c_k^2 I_2 + c_k^3 I_3. \quad (3)$$

Here, let  $\mathbf{c}_k = [c_k^1 \ c_k^2 \ c_k^3]^T$  be a set of coefficients of the image  $\mathbf{I}_k$ . Real images, however, do not satisfy Eq.(3), because shadows and specular reflections are observed. The photometric linearization can convert real images to ideal images which perfectly satisfy Eq.(3). The process of the photometric linearization is divided into the following three steps (Fig.3).

**1. Calculation of a set of coefficients**

First, three base images  $\mathbf{I}_1$ ,  $\mathbf{I}_2$ , and  $\mathbf{I}_3$  are selected from among the input images. A set of coefficients  $\mathbf{c}_k$  of the  $k$ -th input image  $\mathbf{I}_k$  is calculated from the intensities in  $\mathbf{I}_1$ ,  $\mathbf{I}_2$ ,  $\mathbf{I}_3$ , and  $\mathbf{I}_k$ .

**2. Photometric linearization of base images**

Next, the base images are linearized for every pixel based on the input images and the coefficients. Let  $\mathbf{i}_p^L = [i_{(1,p)}^L \ i_{(2,p)}^L \ i_{(3,p)}^L]^T$  be a set of intensities in the linearized base images at pixel  $p$ . This process is performed for all pixels, and three base images  $\mathbf{I}_1$ ,  $\mathbf{I}_2$ , and  $\mathbf{I}_3$  are converted into the linearized base images  $\mathbf{I}_1^L$ ,  $\mathbf{I}_2^L$ , and  $\mathbf{I}_3^L$ .

**3. Photometric linearization of all images**

Finally, all input images are linearized. The  $k$ -th input image  $\mathbf{I}_k$  is linearized by the linear combination of the linearized base images  $\mathbf{I}_1^L$ ,  $\mathbf{I}_2^L$ , and  $\mathbf{I}_3^L$  using  $\mathbf{c}_k$ . We denote the linearized  $\mathbf{I}_k$  as  $\mathbf{I}_k^L$ .

### 3.3 Calculation of Candidates by Random Sampling

The coefficients of the linear combination and the base images have to be determined to satisfy Eq.(3). If we calculate them by minimizing root mean square errors, input images are not converted to ideal images that include only diffuse factor because of shadows and specular reflections.

The photometric linearization solves this problem by the RANSAC-based approach. A lot of candidates are iteratively calculated by random sampling, and the correct value calculated from only diffuse reflections is selected from among the candidates. If all pixels are sampled from the diffuse reflection region, the correct value, which is not affected by specular reflections and shadows, is calculated. That is, we can regard the photometric linearization as a problem to find one correct value calculated by only diffuse reflection factors from among a lot of candidates.

In order to calculate a candidate of the coefficients, three pixels are randomly selected from base images  $\mathbf{I}_1$ ,  $\mathbf{I}_2$ ,  $\mathbf{I}_3$ , and each input image  $\mathbf{I}_k$ . Note that same pixels are selected from every image. A set of coefficients  $\hat{\mathbf{c}}_k$  is calculated from the intensities of the pixels. By the iteration of this process, a lot of candidate coefficients are obtained.

On the other hand, in order to calculate a candidate of the linearized intensities, three images are randomly selected from the input images. If the coefficients  $\mathbf{c}_k$  have already been correctly calculated, the intensities  $\hat{\mathbf{i}}_p^L$  in the linearized base images at pixel  $p$  can be easily calculated. By the iteration of this process, a lot of candidate intensities of the linearized base images are obtained.

### 3.4 Introducing the Criterion for Classification

In order to find a correct value from the numerous candidates calculated by iteration of random sampling, the previous method[12] iterates the estimation of the center of gravity and outlier elimination. However, the algorithm based on a principle of majority has weaknesses. Since the center of gravity may be affected by outliers, an incorrect candidate may be selected because of shadows. So the process tends to be unstable.

Now we propose a new algorithm which can accurately determine the correct value from the numerous candidates. Let's consider the reason why candidates become isolated outliers. That is, we have to check the photometric factors of inliers and outliers. Therefore, we introduce the criterion for classification into the photometric linearization process.

If a candidate is correct, each pixel is classified into the defined factors ( $D$ ,  $S$ ,  $A$ , and  $C$ ) by Eq.(2). Any pixel is never classified into the undefined factor ( $U$ ). Each candidate is evaluated based on the number of pixels which are classified into the defined factors. The candidate which has the maximum number of pixels can be regarded as the correct value.

Basically, the evaluation is based on the defined factors. The specular reflections are, however, excepted from the defined factors. The specular reflection occupies a large area in Fig.(2). If we regard  $S$  as the defined factor, incorrect candidates may be accepted. Since the size of the specular region is relatively small in images, we can ignore specular factors in this evaluation. Hence, we evaluate pixels that are classified into diffuse reflection, attached shadow, and cast shadow by

$$Classifiable(k, p) = \begin{cases} 1 & \text{if } (Region(k, p) = D \cup A \cup C) \\ 0 & \text{if } (Region(k, p) = S \cup U) \end{cases} \quad (4)$$

### 3.5 Evaluation of Candidates

In this section, we present the detailed algorithm to evaluate candidates. For each candidate  $\hat{\mathbf{c}}_k$  of a set of coefficients, the  $k$ -th input image  $\mathbf{I}_k$  is linearized to  $\mathbf{I}_k^L$  by the linear combination of the three base images  $\mathbf{I}_1$ ,  $\mathbf{I}_2$ , and  $\mathbf{I}_3$ . If  $\hat{\mathbf{c}}_k$  is correct, Eq.(4) becomes 1 for almost all pixels. Hence, we define the following function to evaluate candidates of the coefficients  $\hat{\mathbf{c}}_k$ .

$$Support^C(k) = \sum_p Classifiable(k, p) \quad (5)$$

On the other hand, the linearized intensities  $i_{(k,p)}^L$  are calculated by the linear combination using coefficients  $\mathbf{c}_k$  for each candidate  $\hat{\mathbf{i}}_p^L$ . If  $\hat{\mathbf{i}}_p^L$  is correct, Eq.(4) becomes 1 for almost all input images. Hence, we define the following function to evaluate candidates of the linearized intensities.

$$Support^L(p) = \sum_k Classifiable(k, p) \quad (6)$$

The  $Support^C(k)$  and  $Support^L(p)$  are used to calculate the number of pixels which are classified into valid factors. We can regard the candidates for which the function  $Support^C(k)$  or  $Support^L(p)$  returns the maximum as the correct value. By using the estimated coefficients  $c_k$  and intensities  $i_p^L$  in the linearized base images, the accuracy of the photometric linearization can be improved.

### 3.6 Comparison with the previous method [12]

It is noted that the proposed method takes the physical photometric phenomena into account, and considers the photometric factors of outliers, while the previous method [12] is based on only the statistical framework. Therefore, the accuracy can be improved especially in shadow regions.

One may think that if we simply modify [12] so that pixels below the threshold  $T_s$  are excluded as outliers, the accuracy can be improved. By ignoring dark regions, similar results may be acquired. However, the new method can analyze the reason of shadows and classify the outliers into two types of shadow.

## 4 Experimental Results

For the experiments, we used three kinds of materials that have different reflection properties. A ceramic cup (Fig.4) is an example of rough glossy objects, a pot (Fig.7) is an example of very shiny objects, and a marble sphere (Fig.8) is an example of complex reflections such as sub-surface scattering.

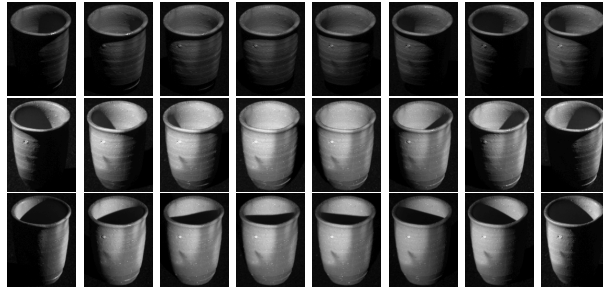
### 4.1 Photometric Classification

We took twenty-four images under various lighting directions in a darkroom keeping a halogen light away from the ceramic cup as shown in Fig.4. Since this cup has a concave surface, some pixels are not illuminated in a number of the input images.

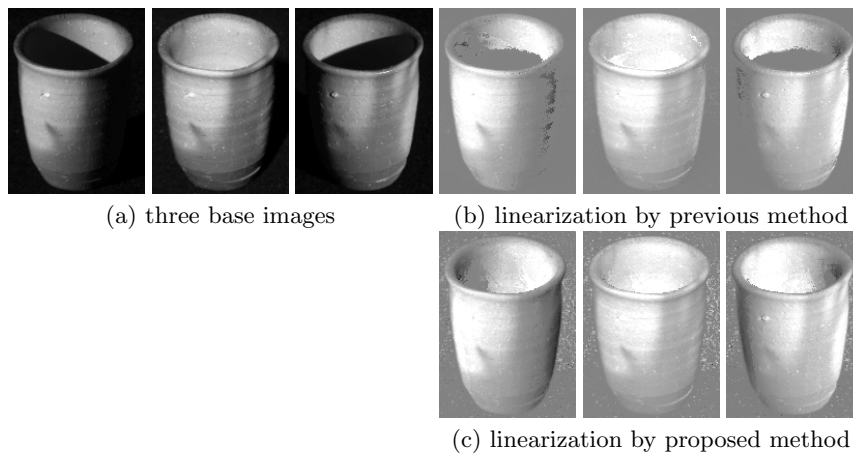
Figure 5 shows three base images selected from input images. (a) shows original base images. (b) and (c) show the results of the photometric linearization. Since the linearized images have negative values, a zero level is expressed as a gray intensity. (b) shows the results of the previous method. Many pixels are incorrectly linearized to be zero, because the previous method is strongly affected by cast shadows. (c) shows the results of the new method based on the classification criterion. We can see that the base images are correctly linearized even if some pixels are not illuminated in a number of the input images.

Figure 6 shows the results of the photometric classification. (a) is an input image, and (b) is the linearized image. Comparing (a) and (b), each pixel was classified into (c) diffuse reflections, (d) specular reflections, (e) attached shadows, and (f) cast shadows. Although attached shadows and cast shadows cannot be classified by a simple threshold, the proposed method can distinguish them.

Next, we applied our method to a glossy object having complex shape. Figure 7(a) shows an example of twenty-four images. (b) is the result of the photometric



**Fig. 4.** Input images taken under various lighting directions (cup: twenty-four images).



**Fig. 5.** Linearized base images.

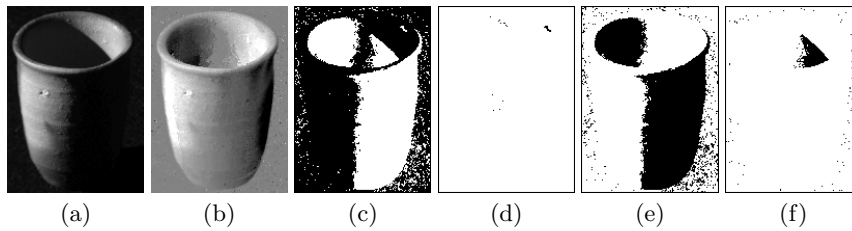


**Fig. 6.** Classification results of the photometric factors (cup). (a): an input image, (b): linearized image, (c): diffuse reflections, (d): specular reflections, (e): attached shadows, (f): cast shadows.

linearization. (c), (d), (e), and (f) show the results of classification as diffuse reflections, specular reflections, attached shadows, and cast shadows, respectively. Each pixel can be classified into a suitable photometric factor even if the target object has a complex shape.

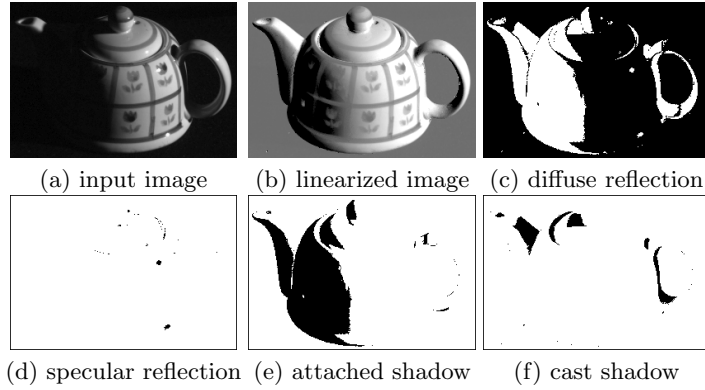


Fig. 7. Classification results of a glossy pot.

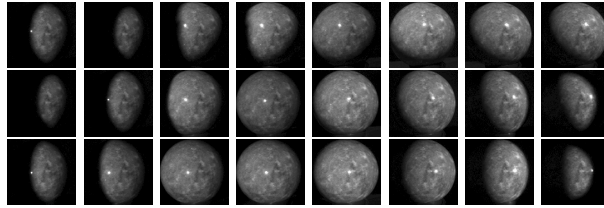


Fig. 8. Input images taken under various lighting directions (sphere).

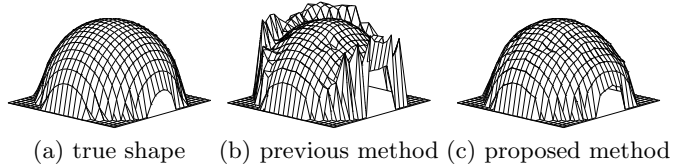


Fig. 9. Reconstructed 3-D shapes.

## 4.2 Photometric Stereo

Next, we show that the photometric linearization can be used for the preprocess of the photometric stereo[1]. We took twenty-four images of a marble sphere under various lighting directions (Fig.8). A part of the surface is not illuminated by obstacles, and complex reflections including subsurface scattering are observed.

After the photometric linearization, the 3-D shape was reconstructed by photometric stereo. Because the lighting directions are unknown, the surface normals cannot be uniquely determined[13]. Therefore, the surface normals are adjusted by the affine transformation to be symmetric around the center of the sphere. Fig.9(a) is a true shape obtained by manual measurement, (b) and (c) are the reconstructed shapes by the previous method and the proposed method, respectively. The previous method failed in the reconstruction due to shadows. On the other hand, new method can correctly linearize and reconstruct at the entire sphere. This result indicates that the photometric linearization method can be applied to objects which have complex BRDFs.

## 5 Conclusions

In this paper, we proposed a new photometric classification method based on the photometric linearization. While the photometric linearization was originally proposed for generating images under the arbitrary lighting direction, we showed that the method can also be used for the classification of photometric factors. We have improved the accuracy of the photometric linearization method by introducing the classification criterion into the linearization process.

The photometric linearization has an important role as a fundamental technique of computer vision such as photometric stereo and shape-from-shading. We confirmed that our method can be applied for a variety of materials, and that the photometric stereo becomes robust to shadows by applying the photometric classification as a preprocessing. In the future, we intend to analyze more complex factors such as interreflection.

This research was supported by the Ministry of Education, Science, Sports and Culture, Grant-in-Aid for Young Scientists (A), 17680018.

## References

1. R.J.Woodham: Photometric Stereo, MIT AI Memo, (1978).
2. S.Shafer: Using color to separate reflection components, Color Research and Applications, Vol.10, pp.210-218, (1985).
3. G.Klinker, S.Shafer and T.Kanade: The measurement of highlights in color images, IJCV, Vol.2, No.1, pp.7-32, (1988).
4. Y.Sato and K.Ikeuchi: Temporal-color space analysis of reflection, JOSA A, Vol.11, No.7, pp.2990-3002, (1994).
5. Y.Sato, M.Wheeler and K.Ikeuchi: Object Shape and Reflectance Modeling from Observation, Proc. SIGGRAPH'97, pp.379-387, (1997).
6. L.B.Wolff and E.Boult: Constraining Object Features Using a Polarization Reflectance Model, IEEE Trans. PAMI, Vol.13, No.7, pp.635-657, (1991).
7. S.K. Nayar, X. Fang and T.E. Boult: Removal of specularities using color and polarization, Proc. CVPR'93, pp.583-590, (1993).
8. K.Ikeuchi and K.Sato: Determining Reflectance Properties of an Object Using Range and Brightness Images, IEEE Trans. PAMI, Vol.13, No.11, pp.1139-1153, (1991).
9. A.Shashua: Geometry and Photometry in 3D Visual Recognition, Ph.D thesis, Dept. Brain and Cognitive Science, MIT, (1992).
10. P.N.Belhumeur and D.J.Kriegman: What is the Set of Images of an Object Under All Possible Lighting Conditions?, Proc. CVPR'96, pp.270-277, (1996).
11. A.S.Georghiades, D.J.Kriegman and P.N. Belhumeur: From Few to Many: Illumination Cone Models for Face Recognition Under Variable Lighting and Pose, IEEE Trans. PAMI, Vol.23, No.6, pp.643-660, (2001).
12. Y.Mukaigawa, H.Miyaki, S.Mihashi and T.Shakunaga: Photometric Image-Based Rendering for Image Generation in Arbitrary Illumination, Proc. ICCV2001, pp.652-659, (2001).
13. P.N.Belhumeur, D.J.Kriegman and A.L.Yuille: The bas-relief ambiguity, Proc. CVPR'97, pp.1060-1066, (1997).